Erratum: Exclusive photoproduction of a $\gamma\,\rho$ pair with a large invariant mass

R. Boussarie,[a,1] **B. Pire,**[b] **L. Szymanowski**[c] **and S. Wallon**[a,d]

[a] *LPT, Université Paris-Sud, CNRS, Université Paris-Saclay,*
91405, Orsay, France

[b] *Centre de Physique Théorique, Ecole polytechnique, CNRS, Université Paris-Saclay,*
91128 Palaiseau, France

[c] *National Center for Nuclear Research (NCBJ),*
00681 Warsaw, Poland

[d] *UPMC Univ. Paris 06, Faculté de physique,*
4 place Jussieu, 75252 Paris Cedex 05, France

E-mail: renaud.boussarie@th.u-psud.fr,
bernard.pire@polytechnique.edu, Lech.Szymanowski@ncbj.gov.pl,
wallon@th.u-psud.fr

ERRATUM TO: JHEP02(2017)054

ABSTRACT: An unfortunate misprint in our numerical code has led to an overestimate of the cross section for the exclusive photoproduction of a $\gamma\,\rho_L$ pair in the kinematics where the pair has a large invariant mass and the final nucleon has a small transverse momentum, described in the collinear factorization framework. The rates are thus expected to be smaller but the possibility to disentangle the transversity GPDs through the process where the $\rho-$meson is transversely polarized is enhanced.

---

[1] Present address: Institute of Nuclear Physics, Polish Academy of Sciences, Radzikowskiego 152, PL-31-342 Kraków, Poland. E-mail: renaud.boussarie@ifj.edu.pl.
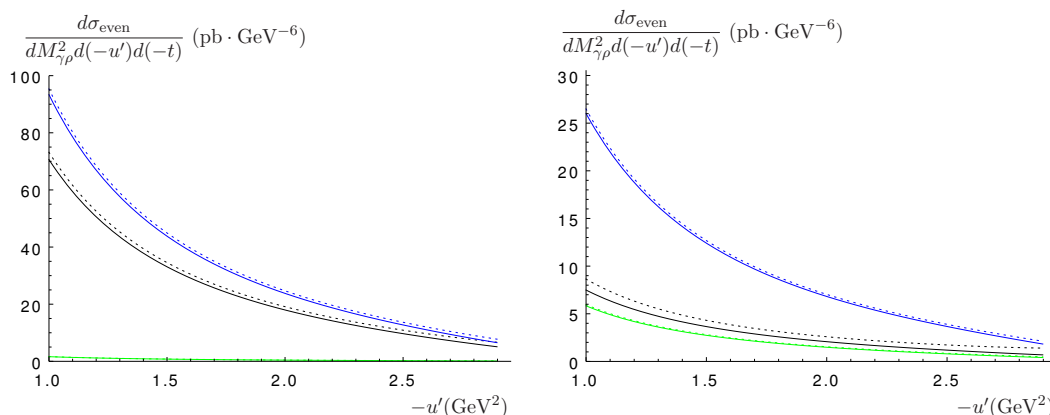
Figure 6. Differential cross section for a photon and a longitudinally polarized ρ meson production, for the proton (left) and the neutron (right), at $M_{\gamma\rho}^2 = 4\ \text{GeV}^2$. Both vector and axial GPDs are included. In black the contributions of both u and d quarks, in blue the contribution of the u quark, and in green the contribution of the d quark. Solid: "valence" model, dotted: "standard" model. This figure shows the dominance of the u-quark contribution due to the charge effect. Note that the interference between $u-$quark and $d-$quark contributions is important and negative.
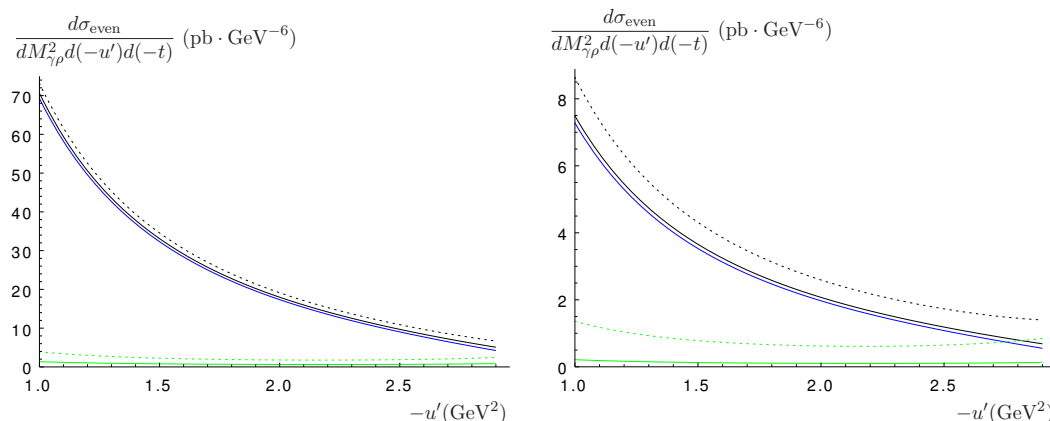

Figure 7. Differential cross section for a photon and a longitudinally polarized ρ meson production, for the proton (left) and the neutron (right), at $M_{\gamma\rho}^2 = 4\ \text{GeV}^2$. Both u and d quark contributions are included. In black the contributions of both vector and axial amplitudes, in blue the contribution of the vector amplitude, and in green the contribution of the axial amplitude. Solid: "valence" model, dotted: "standard" model. This figure shows the dominance of the vector GPD contributions. There is no interference between the vector and axial amplitudes.

In our published paper [1], an unfortunate misprint in our numerical code has led to an overestimate of the cross section for the exclusive photoproduction of a $\gamma\,\rho$ pair, in the case where the final ρ-meson is longitudinally polarized. The corrected plots corresponding to figures 6-11, 16 and 22 are displayed below, and can be obtained from the previous figures by a division by a factor of 36. The total rates are thus expected to be smaller but the possibility to disentangle the transversity GPDs through the process where the $\rho-$meson is transversely polarized is enhanced.
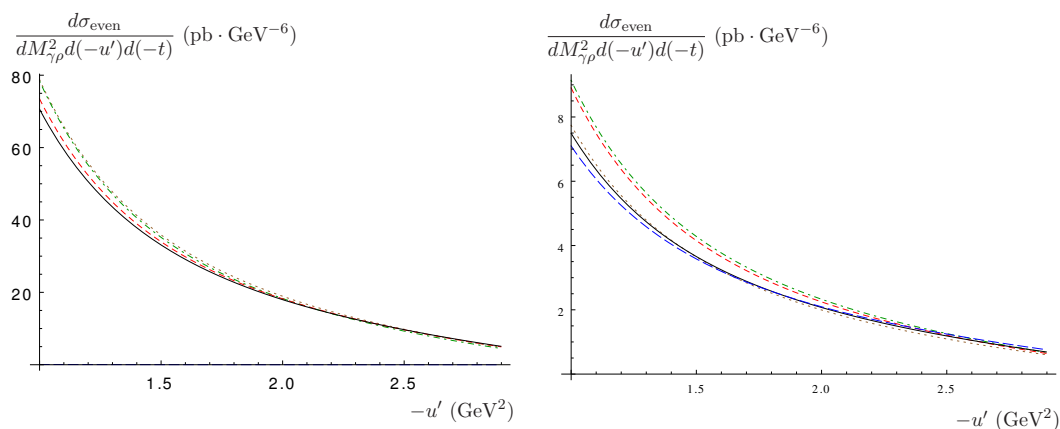
$$\frac{d\sigma_{\text{even}}}{dM_{\gamma\rho}^2 d(-u')d(-t)} \text{ (pb} \cdot \text{GeV}^{-6})$$

$$\frac{d\sigma_{\text{even}}}{dM_{\gamma\rho}^2 d(-u')d(-t)} \text{ (pb} \cdot \text{GeV}^{-6})$$

$-u'$ (GeV^2)

$-u'$ (GeV^2)

Figure 8. Differential cross section for a photon and a longitudinally polarized ρ meson production, for the proton (left) and the neutron (right), as a function of $-u'$, for $M_{\gamma\rho}^2 = 4$ GeV^2. The various curves differ with respect to the ansätze for the PDFs q, and thus for the GPDs H^u and H^d: GRV-98 (solid black), MSTW2008lo (long-dashed blue), MSTW2008nnlo (short-dashed red), ABM11nnlo (dotted-dashed green), CT10nnlo (dotted brown).
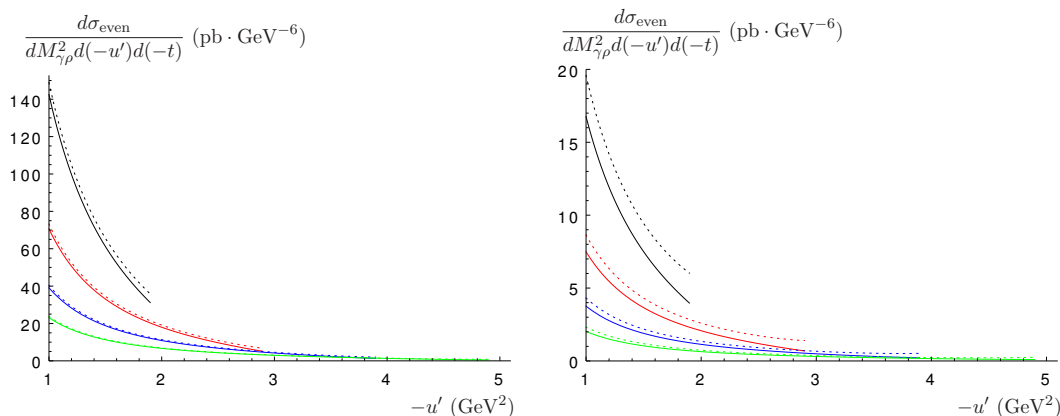
$$\frac{d\sigma_{\text{even}}}{dM_{\gamma\rho}^2 d(-u')d(-t)} \text{ (pb} \cdot \text{GeV}^{-6})$$

$$\frac{d\sigma_{\text{even}}}{dM_{\gamma\rho}^2 d(-u')d(-t)} \text{ (pb} \cdot \text{GeV}^{-6})$$

$-u'$ (GeV^2)

$-u'$ (GeV^2)

Figure 9. Differential cross section for a photon and a longitudinally polarized ρ meson production, for the proton (left) and the neutron (right), as a function of $-u'$, for $M_{\gamma\rho}^2 = 3, 4, 5, 6$ GeV^2 (resp. in black, red, blue, green). Solid: "valence" model, dotted: "standard" model.
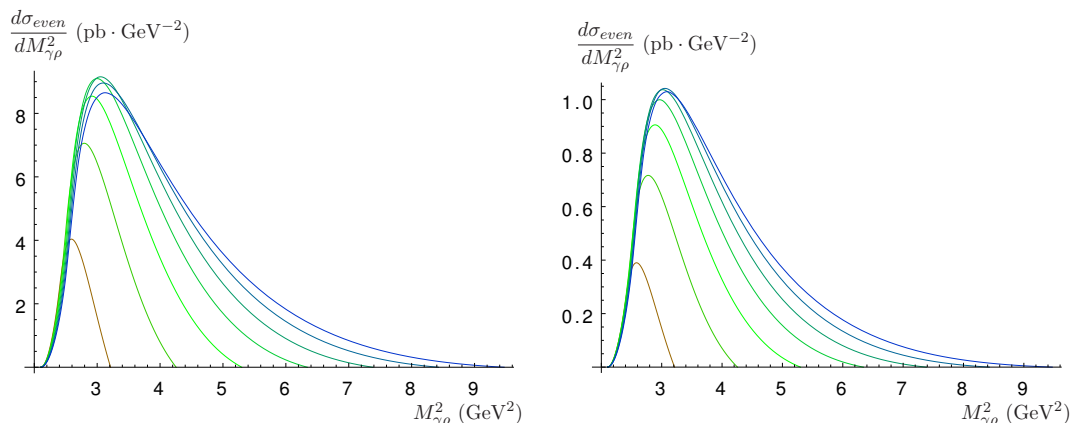
u

Figure 10. Differential cross section $d\sigma/dM_{\gamma\rho}^2$ for a photon and a longitudinally polarized ρ meson production, on a proton (left) or neutron (right) target. The values of $S_{\gamma N}$ vary in the set 8, 10, 12, 14, 16, 18, 20 GeV^2. (from 8: left, brown to 20: right, blue), covering the JLab energy range. We use here the "valence" scenario.
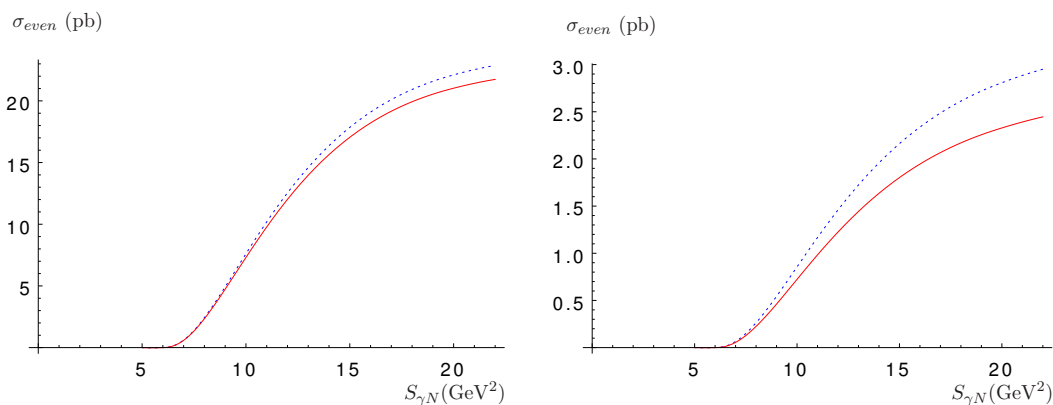

Figure 11. Integrated cross section for a photon and a longitudinally polarized ρ meson production, on a proton (left) or neutron (right) target. The solid red curves correspond to the "valence" scenario while the dashed blue curves correspond to the "standard" one.
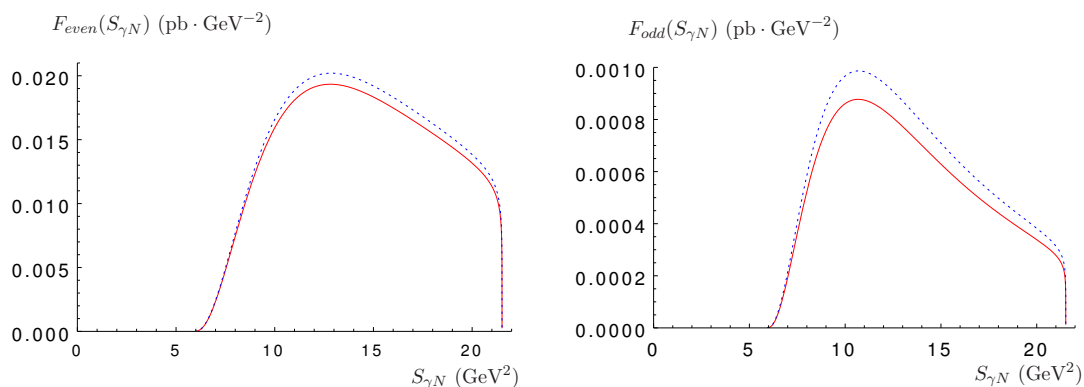

Figure 16. Shape of the integrand of σ_{eN}, as a function of the invariant mass of the hadronic produced state, on a proton target. Left: longitudinally polarized ρ meson production. Right: transverse ρ meson production. In solid-red: "valence". In dashed-blue: "standard".
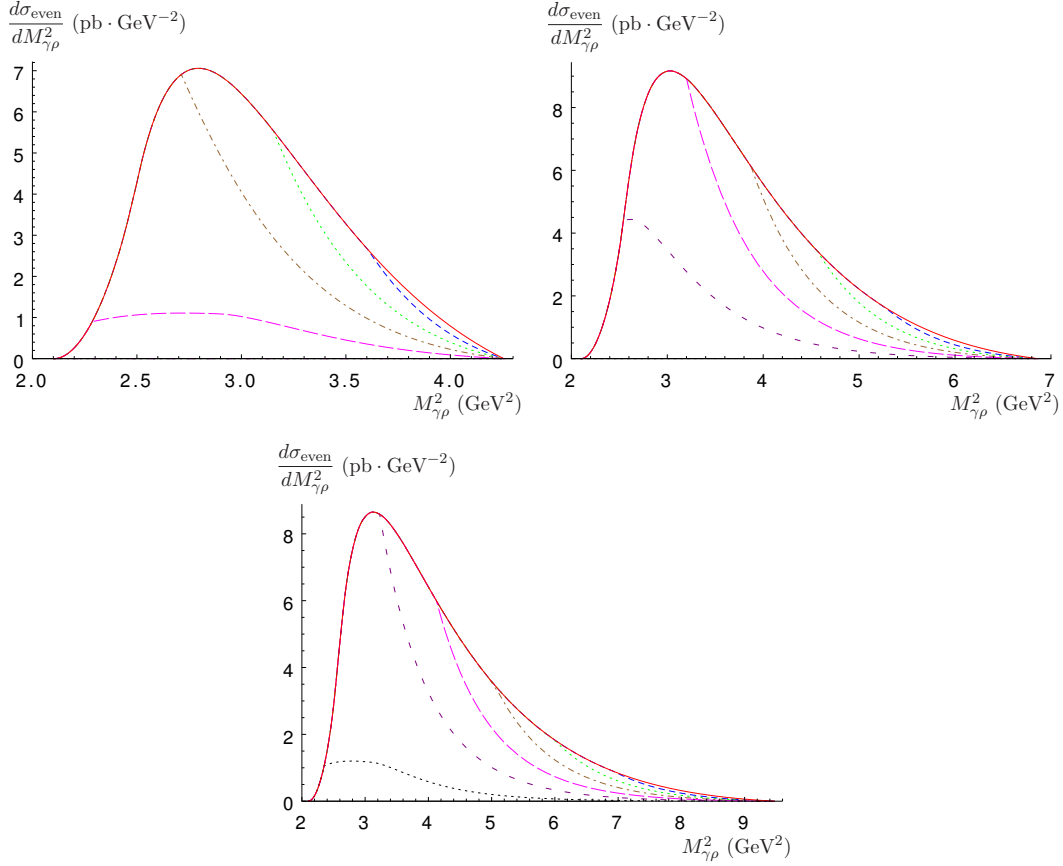
Figure 22. The differential cross section $\frac{d\sigma_{\text{even}}}{dM_{\gamma\rho}^2}$. Solid red: no angular cut. Other curves show the effect of an upper angular cut θ for the out-going γ: 35° (dashed blue), 30° (dotted green), 25° (dashed-dotted brown), 20° (long-dashed magenta), 15° (short-dashed purple) and 10° (dotted black). Up, left: $S_{\gamma N} = 10 \text{ GeV}^2$. Up, right: $S_{\gamma N} = 15 \text{ GeV}^2$. Down: $S_{\gamma N} = 20 \text{ GeV}^2$.

Additional corrections (the modifications on the equations have no effect on our estimates), are:

- Equation (4.11) should be replaced by

$$
\begin{aligned}
T_{A_5} &= (p_\perp \cdot \varepsilon_{k\perp}^*)\, \epsilon^{n\, p\, \varepsilon_{q\perp}\, p_\perp}, \\
T_{B_5} &= -(p_\perp \cdot \varepsilon_{q\perp})\, \epsilon^{n\, p\varepsilon_{k\perp}^*\, p_\perp}.
\end{aligned}
\tag{4.11}
$$

- In equations (4.10) and (A.10)–(A.18), T_{A_5} should be replaced by $-T_{A_5}$.

- In equation (4.12), and (4.13), the r.h.s. should be multiplied by 2.

- Equation (5.19) should read:

$$
\begin{aligned}
|\overline{\mathcal{M}}^{CE}|^2 = \frac{4}{s^2}(1-\xi^2)\left(C^{u\,CE}\right)^2 \Bigg\{ &2\left|N_A^u - \frac{1}{4}N_A^d\right|^2 + \frac{p_\perp^4}{s^2}\left|N_B^u - \frac{1}{4}N_B^d\right|^2 \\
&+ \frac{p_\perp^2}{s}\left(\left[N_A^u - \frac{1}{4}N_A^d\right]\left[N_B^u - \frac{1}{4}N_B^d\right]^* + \text{c.c.}\right) \\
&+ \frac{p_\perp^4}{4s^2}\left|\tilde{N}_A^u - \frac{1}{4}\tilde{N}_A^d\right|^2 + \frac{p_\perp^4}{4s^2}\left|\tilde{N}_B^u - \frac{1}{4}\tilde{N}_B^d\right|^2 \Bigg\}.
\end{aligned}
\tag{5.19}
$$

$$- 4 -$$

- The first sentence of subsection 5.5 should be:

  For $S_{\gamma N} = 20$ GeV^2, the integration over $M_{\gamma\rho}^2$ of our above results within our allowed kinematical region, here 2.10 GeV^2 $<$ $M_{\gamma\rho}^2$ $<$ 9.47 GeV^2 (see appendix D), allows to obtain the cross sections $\sigma_{\text{odd}}^{\text{proton}} \simeq 0.54$ pb and $\sigma_{\text{even}}^{\text{proton}} \simeq 21$ pb for the proton, and $\sigma_{\text{odd}}^{\text{neutron}} \simeq 0.42$ pb and $\sigma_{\text{even}}^{\text{neutron}} \simeq 2.3$ pb for the neutron.

- The last sentence of section 6 should read:

  With an expected luminosity $\mathcal{L} = 100$ nb$^{-1}s^{-1}$ we obtain for 100 days of run: 7.5 10^3 ρ_T and 1.9 10^5 ρ_L.

- In the conclusion, the beginning of the last but one paragraph should read:

  To conclude, the cross section of our process is a factor 10 more than the $\gamma P \to P e^+ e^-$ process, for similar values of the hard scale, for which experimental proposals have been approved at JLab.

- The r.h.s. of equations (B.26)–(B-39) and (B.45)–(B-64) should be multiplied by 6.

- Equation (D.11) should read

$$\frac{d\sigma}{dM_{\gamma\rho}^2} = \frac{C^4}{3}\left[\theta(M_{\gamma\rho\,\text{crit}}^2 < M_{\gamma\rho}^2 < M_{\gamma\rho\,\text{trans}}^2)\right.$$

$$\times \int_{(-u')_{\text{min}}}^{(-u')_{\text{maxMax}}} d(-u') \left[\frac{1}{(-(-t)_{\text{max}} - C)^3} - \frac{1}{(-(-t)_{\text{min}}(-u') - C)^3}\right]$$

$$\times \left.\frac{d\sigma}{dM_{\gamma\rho}^2 d(-u')d(-t)}\right|_{(-t)_{\text{min}}} + \theta(M_{\gamma\rho\,\text{trans}}^2 < M_{\gamma\rho}^2 < M_{\gamma\rho\,\text{Max}}^2)$$

$$\times \left\{\left[\frac{1}{(-(-t)_{\text{max}} - C)^3} - \frac{1}{(-(-t)_{\text{min}} - C)^3}\right]\right.$$

$$\times \int_{(-u')_{\text{min}}}^{(-u')_{\text{maxMin}}} d(-u') \left.\frac{d\sigma}{dM_{\gamma\rho}^2 d(-u')d(-t)}\right|_{(-t)_{\text{min}}}$$

$$+ \int_{(-u')_{\text{maxMin}}}^{(-u')_{\text{maxMax}}} d(-u') \left[\frac{1}{(-(-t)_{\text{max}} - C)^3} - \frac{1}{(-(-t)_{\text{min}}(-u') - C)^3}\right]$$

$$\times \left.\left.\left.\frac{d\sigma}{dM_{\gamma\rho}^2 d(-u')d(-t)}\right|_{(-t)_{\text{min}}}\right\}\right],$$

(D.11)

- Equation (E.2) and (E.6) should read

$$\tan\theta = -\frac{2Ms(1+\xi)\alpha \parallel \vec{p}_t - \frac{\vec{\Delta}_t}{2} \parallel}{-\alpha^2(1+\xi)^2 s^2 + (\vec{p}_t - \frac{\vec{\Delta}_t}{2})^2 M^2}\,.$$

(E.2)

and

$$\tan\theta = -\frac{2Ms(1+\xi)\alpha\, p_t}{-\alpha^2(1+\xi)^2 s^2 + \vec{p}_t^2 M^2}\,.$$

(E.6)

- The last sentences of the paper should read:

  Putting additional cuts on $M_{\gamma\rho}^2$, like $M_{\gamma\rho}^2 > 6$ GeV^2, allows to increase the ratio odd versus even from $\sim 1/25$ to $\sim 2/3$, keeping about 3% of the chiral-odd contribution, for typically $S_{\gamma N}$ between $18\,\text{GeV}^2$ and the maximal value $21.5\,\text{GeV}^2$. This in principle would lead, dealing with observables sensitive to the interference between the chiral-odd and the chiral-even contributions, to a relative signal of the order of 80%.

References

[1] R. Boussarie, B. Pire, L. Szymanowski and S. Wallon, *Exclusive photoproduction of a $\gamma\,\rho$ pair with a large invariant mass*, *JHEP* **02** (2017) 054 [arXiv:1609.03830] [INSPIRE].